New algorithm for weak changes detection with application to welding electrical signals

Youssef Salman, Anis Hoayek, Mireille Batton-Hubert

New algorithm for weak changes detection with application to welding electrical signals

Youssef Salman* · **Anis Hoayek** · **Mireille Batton-Hubert**

Received: date / Accepted: date

Abstract We propose a new algorithm for detecting weak changes in the mean of a class piece-wise stationary CHARN models. Through a simulation experiment, we establish the efficacy and precision of the new algorithm in detecting weak changes in the mean and accurately estimating their locations. Furthermore, we illustrate the robust performance of our algorithm through its application to welding electrical signals (WES).

Keywords Weak changes, CHARN models, Change-points, Welds.

Mathematics Subject Classification (2020) 62F05, 62J20, 62M02, 62M05, 62M10, 62P30

1 Introduction

The analysis of structural change-points, or breaks, has begun by Page (1954) in quality control, but over time, it has expanded to include a strong statistical component in a various fields, such as economics (Perron et al. (2006)), climatology (Reeves et al. (2007) and Beaulieu et al. (2012)), finance (Andreou and Ghysels (2009)) and engineering (Stoumbos et al. (2000)).
The changes in time series may take different form depending on the magnitude of changes. From time series vision, it can be visible (non small magnitude of change in the parameters of the considered model) or approximately hidden (weak magnitude). Even if the magnitude is considerable, it may occurs just for few number of observations, we call it in this paper as a false alarm (or an anomaly in the data). Otherwise, when the changes occur and continue for a while, the data take the form of piece-wise stationary data which is the case we consider it here.
In this paper, we use the theoretical results obtained in Salman (2022) and we introduce a new algorithm for detecting weak changes in the mean. We examine the performance of the proposed algorithm using a simulated data and we apply it to a real data set such as welding electrical signals. The new algorithm is motivated by the reduction of the effect of the white noise from which sometimes it can be detected as a change-point using the algorithm of Salman (2022). At the same time, the new one contains some techniques for identifying the type of the changes detected and the distinction between an anomaly (false alarm) and true change-point. This distinction we get by monitoring the power of the test calculated around the observation under testing. The simulated data presented in this paper shows the efficiency and accuracy of this new algorithm, and it validate the good performance for identifying the change faced.
This paper is categorized as follow. In Section 2, we go back to some works on change-points presented in literature. In Section 3, we recall the essential theoretical results of Salman (2022). These results are used in Section 4 for constructing the new algorithm. In section 5, a simulation experiment is conducted for the

Y. Salman, Corresponding author,
Mines Saint-Etienne, Univ Clermont Auvergne, CNRS, UMR 6158 LIMOS, Institut Henri Fayol, F - 42023 Saint-Etienne France
E-mail: youssef.salman@emse.fr

A. Hoayek
Mines Saint-Etienne, Univ Clermont Auvergne, CNRS, UMR 6158 LIMOS, Institut Henri Fayol, F - 42023 Saint-Etienne France
E-mail: anis.hoayek@emse.fr

M. Batton-Hubert
Mines Saint-Etienne, Univ Clermont Auvergne, CNRS, UMR 6158 LIMOS, Institut Henri Fayol, F - 42023 Saint-Etienne France
E-mail: batton-hubert@emse.fr

application of our algorithm. In Section 6, an application to a real data set is done. Section 7 concludes the paper.

2 Bibliography

One of the statistics most often used for the segmentation of the time series is the CUSUM test, introduced by Page (1954). Brown et al. (1975) introduce another version of CUSUM test based on the least-squares residuals, denoted by CUSUM^{ols}. Zeileis (2001) and Zeileis (2004) use the CUSUM test in order to estimate the p-value. They bounded the p-value with two approximate bounds for the standard CUSUM test and CUSUM^{ols} test. One of the major drawbacks is that they have low power, when the changes occur at the beginning or when they occur at the end (late changes). For this reason, they update the bounds, see Zeileis (2001) and Zeileis (2004). Later, many version of CUSUM test was introduced, see Horváth et al. (2020). Aue and Horváth (2013) shows how procedures based on the popular cumulative sum, CUSUM, statistics can be modified to work also for data exhibiting serial dependence. If the data allows for parametric modeling, the authors demonstrate how likelihood approaches may be utilized to recover structural breaks. The structural breaks in the conditional mean, variance, and second-order characteristics are studied.
The literature on change-points is large and various. Depending on whether the data are given in advance or acquired sequentially, we can classify the change-point detection as off-line or on-line respectively. In the off-line multiple-change-point estimation, a common approach involves searching for the set of breaks that optimizes certain objective functions like Bayes information criterion BIC or least squares criterion see,e.g. Yao (1987) and Horváth (1993). Since the number of change-points combinations grows exponentially as the sample size grows, the optimization can be extremely computationally expensive. For that, several methods have been suggested, such as the purned exact linear time (PELT) of Killick et al. (2012) and genetic algorithm of Davis et al. (2006), and the optimization remains difficult. To pass around the difficulty in optimization, one can find the binary segmentation method, which started by Vostrikova (1981).
Cho and Fryzlewicz (2012) apply the binary segmentation method on wavelet periodograms and develop a method to detect change-points in the covariance structure of a piece-wise stationary, linear time series with an unknown number of breakpoints. An important updated version of binary segmentation method called Wild binary segmentation (WBS), is introduced by Fryzlewicz (2014) for detecting changes in the mean. Korkas and PryzlewiczV (2017) extend the idea for detecting change in covariance structure of time series.

Yau and Zhao (2016) propose a likelihood ratio scan method for estimating change points in piece-wise stationary processes. The authors use scan statistics to reduce the computationally infeasible global multiple-change-point estimation problem to a number of single-change-point detection problems in various local windows. The authors establish the consistency for the estimated numbers and locations of the change-points.
In the context of time series, very few is done about testing no change against local alternatives of weak changes. We mean by weak changes those of small magnitudes. Ltaifa (2021) and Ngatchou-Wandji and Ltaifa (2021) study this problem for the case of testing the mean of Conditional Heteroscedastic Autoregressive Nonlinear "CHARN" model . Salman (2022) extends the work of Ltaifa (2021) to more general models. In this paper, we use the theoretical results obtained in Salman (2022), and we introduce a new algorithm for detecting weak changes in the mean and identifying their types.

3 Model, problematic, and main results of Salman (2022)

In this section, we recall, in a briefly way, the method developed in Salman (2022) from which it is a generalization of that presented in Ltaifa (2021) and Ngatchou-Wandji and Ltaifa (2021). These methods are constructed for detecting weak changes in the mean based on the theoretical power of a likelihood ratio test. The class of the statistical model presented in Salman (2022) is the Conditional Heteroscedastic Autoregressive Nonlinear model "CHARN" (see, e.g., Härdle et al. (1998)).
More precisely, let $d, p, k, n \in \mathbb{N}$ and $k << n$. Assume the observations $X_1, \ldots, X_n$ issued from the following piece-wise stationary CHARN model

$$X_t = T(\boldsymbol{\rho_0} + \boldsymbol{\gamma} \odot \omega(t); \mathbf{X}_{t-1}) + V(\mathbf{X}_{t-1})\varepsilon_t, t \in \mathbb{Z}, \tag{31}$$

with

$$X_t = Y_{t,j} = T(\boldsymbol{\rho_0} + \boldsymbol{\gamma}_j \omega_j(t); \mathbf{X}_{t-1,j}) + V(\mathbf{X}_{t-1,j})\varepsilon_t, \quad \tau_{j-1} \leq t < \tau_j, \quad j = 1, \ldots, k+1, \tag{32}$$

where for $j = 1, \ldots, k$, $(Y_{t,j})_{t\in\mathbb{Z}}$ is a stationary and ergodic process; $\boldsymbol{\rho}_0 \in \mathbb{R}^p$, $T(\boldsymbol{\rho}_0, .)$ and $V(.)$ are real-valued functions with $\inf_{x\in\mathbb{R}^d} V(x) > 0$; the τ_j, $j = 0, \ldots, k+1$, are potential instants of changes with

$\tau_0 = 1$ and $\tau_{k+1} = n+1$; for $j = 1, \ldots, k$, $\mathbf{X}_{t,j} = (Y_{t,j}, \ldots, Y_{t-d+1,j})^\top$, $\mathbf{X}_{\tau_{j-1}+\ell} = \mathbf{X}_{\tau_{j-1}+\ell,j}$, $\ell = 0, \ldots, d-1$ and for $t \in [\tau_{j-1} + d - 1, \tau_j)$, $\mathbf{X}_t = (X_t, \ldots, X_{t-d+1})^\top$; for $j, \ell = 1, \ldots, k$, $j \neq \ell$, the process $(Y_{t,j})_{t\in\mathbb{Z}}$ and $(Y_{t,\ell})_{t\in\mathbb{Z}}$ are mutually independent (Yau and Zhao (2016) noted that this assumption can be extended to some weak dependence assumption); $(\varepsilon_t)_{t\in\mathbb{Z}}$ is a standard white noise with density f. $\boldsymbol{\gamma} = \left(\boldsymbol{\gamma}_1^\top, \ldots, \boldsymbol{\gamma}_{k+1}^\top\right)^\top$, $\boldsymbol{\gamma}_j \in \mathbb{R}^p$, $j = 1, \ldots, k+1$; $\omega(t) = (\mathbb{1}_{[\tau_0,\tau_1)}(t), \mathbb{1}_{[\tau_1,\tau_2)}(t), ..., \mathbb{1}_{[\tau_{k-1},\tau_k)}(t), \mathbb{1}_{[\tau_k,\tau_{k+1})}(t))^\top = (\omega_1(t), \ldots, \omega_{k+1}(t)) \in \{0,1\}^{k+1}$; for $\boldsymbol{\gamma} = (\boldsymbol{\gamma}_1^\top, \ldots, \boldsymbol{\gamma}_{k+1}^\top)^\top$ and $\omega(t) = (\omega_1(t), \ldots, \omega_{k+1}(t))^\top$, $\boldsymbol{\gamma} \odot \omega(t)$ stands for $\boldsymbol{\gamma} \odot \omega(t) = \boldsymbol{\gamma}_1\omega_1(t) + \cdots + \boldsymbol{\gamma}_{k+1}\omega_{k+1}(t) \in \mathbb{R}^p$, and $\boldsymbol{\gamma}_i\omega_i = (\gamma_{i,1}\omega_i, \ldots, \gamma_{i,p}\omega_i) \in \mathbb{R}^p$.
This category of models is expansive, encompassing a variety of models including AR(p), ARCH(p), EXPAR(p), GEXPAR(p). Statistical and probabilistic properties have been extensively investigated in the existing literature (see, e.g. Chen et al. (2018) for the study of the ergodicity of GEXPAR models).
For $\boldsymbol{\gamma}_0 \in \mathbb{R}^{p(k+1)}$ and $\boldsymbol{\beta} \in \mathbb{R}^{p(k+1)}$ depending on the τ_j's, Salman (2022) construct a likelihood ratio test for testing

$$H_0 : \boldsymbol{\gamma} = \boldsymbol{\gamma}_0 \quad \text{against} \quad H_{\boldsymbol{\beta}}^{(n)} : \boldsymbol{\gamma} = \boldsymbol{\gamma}_n = \boldsymbol{\gamma}_0 + \frac{\boldsymbol{\beta}}{\sqrt{n}}. \tag{33}$$

Note that the norm of $\boldsymbol{\beta}$ is small in front of n, and then the two hypotheses considered are getting closer as the sample size n grows up.
First, the authors prove that the test constructed establish the locally asymptotically normal property (LAN) and the hypotheses considered are contiguous in the sens of Le Cam (see Le Cam (1986) and Droesbeke and Fine (1996)). These properties allow the study of the theoretical power of the test constructed and lead to obtain an explicit expression of it. Indeed, under some technical hypotheses, they prove that the constructed likelihood ratio test is asymptotically optimal and its asymptotic power has the following expression

$$\mathcal{P}_{k,\tau^k} = 1 - \Phi(z_\alpha - \vartheta(\boldsymbol{\rho}_0, \boldsymbol{\gamma}_0, \boldsymbol{\beta})) \tag{34}$$

where

- $\boldsymbol{\rho}_0$ represent the true nuisance parameter and $\alpha \in (0,1)$ represent the level of significance,
- z_α is the $(1-\alpha)$-quantile of the standard Gaussian distribution with cumulative distribution function ϕ,
- ϑ is a real function defined in $\mathbb{R}^{p(k+1)\times p(k+1)}$, where its expression is given in Salman (2022).

In practice, the parameters are unknown and have to be estimated. Many works focus on the estimation of the parameters, for example, Chen et al. (2018) discuss the estimation of the parameters of the linear and non-linear part in GExpAR models which they are particular cases of CHARN model studied in Salman (2022), Brockwell et al. (1990) for linear models as ARMA and many others. A decision for the testing problem considered in Salman (2022) can be taken to be the estimation of the test's power $\widehat{\mathcal{P}}_{k,\tau^k}$ which is the one obtained by replacing the true parameters with their estimators in $\mathcal{P}_{k,\tau^k}$. To explain the techniques used here for parameters estimation, for $1 \leq j \leq k+1$, $1 \leq h \leq p$, let $\widehat{\rho}_{j,h}$ a consistent estimator (for example, the maximum likelihood estimator) of $\rho_{0,h} + \beta_{j,h}/\sqrt{n}$ on the basis of observations within $[\tau_{j-1}, \tau_j)$. Then one can consider $\widehat{\beta}_{j,h} = \sqrt{n}(\widehat{\rho}_{j,h} - \widehat{\rho}_{0,h})$ as an estimator of $\beta_{j,h}$, where $\widehat{\rho}_{0,h}$ is the estimator of the stationary parameter $\rho_{0,h}$ on the basis of the first piece of observation $[1, \tau_1)$. By replacing the parameters with their estimators, the authors prove that the test constructed remains asymptotically optimal and they derived an explicit expression of its power, noted by $\widehat{\mathcal{P}}_{k,\tau^k}$.

4 New algorithm for weak-changes detection and their locations estimation

The time series at hand may has an invisible weak jumps when the parameters of its distribution weakly change at sometime. This type of jumps may cause a visible results in the future. For example, a seismic wave may be the results of a small movement of a small earth plate situated in a sensitive earth location.
As elucidated in Salman (2022), the constructed test possesses the capability to extend beyond its role of testing no change against at least one change. It can be effectively employed to identify concealed changes amidst two or more already detected changes, as determined by certain methodologies. To illustrate, consider a scenario where changes have been pinpointed within the data using a specific approach, and their respective positions have been estimated. This test functions as a screening tool to uncover potential unnoticed changes as suggested by these methodologies. In such a context, the identified changes as well as their locations are assumed to be established. Consequently, the components of $\boldsymbol{\gamma}_0$ cease to remain uniform, and specific τ_j values in the model are deemed as known. Therefore, the test can be leveraged to evaluate the null hypothesis of ι changes against at least $\iota + 1$ changes, where ι is a predetermined natural number.
The algorithm introduced in Salman (2022) may be susceptible to the influence of white noise. To elaborate on this, consider two distinct time intervals, denoted as $[1, t)$ and $[t+1, n)$, where $t \in (1, n)$. Assume that the

parameters of the statistical model remain consistent across both intervals, while the white noise assumes extreme values within one of them. In such a scenario, this algorithm might encounter this situation, leading to the identification of a change. However, due to the absence of techniques capable of discriminating between a genuine change-point and a false alarm, this detected change might be erroneously classified as a change-point.
Here, we introduce a new algorithm motivated by both the reduction of the impact of white noise and the classification of the detected changes into change-points and false alarms. In the sequel, we denote by $\mathcal{P}_{k,\tau^k}$, $k \geq 1$ the theoretical power of the test considered at $\tau^k = (\tau_1, \ldots, \tau_k)$. For $\alpha \in (0,1)$ representing the level of significance, we denote by $\mathcal{P}_{0,\tau^0} = \alpha$ the nominal level of the test.
Let $\zeta \in (0, .1)$ and $X_1, X_2, \ldots, X_m$, $(m << n)$, the m first stationary observations. A crucial point to mention is that, in practice, m will be small than that considered in Salman (2022).

Our procedure for detecting weak changes in the time series $X_1, X_2, \ldots, X_n$ and estimating their locations is described in the following algorithm.

Location 1 :

Put $t = 1$

$(\mathcal{S}_\mathbf{1})$: Consider the two intervals $\mathcal{I}_1$ and $\mathcal{I}_2$ that contains respectively the observations $X_1, \ldots, X_{m+t-1}$ and $X_1, \ldots, X_{m+t}$. So that the difference between the two intervals considered is the single observation X_{m+t} which is under testing.
$(\mathcal{S}_\mathbf{1})'$: **Adjust** model (31) to $\mathcal{I}_1$ and $\mathcal{I}_2$. Then, apply the testing procedure presented in Salman (2022).

If $|\mathcal{P}_{1,t} - \mathcal{P}_{0,\tau^0}| > \zeta$,

Replace X_{m+t} with $X_{m+\varsigma}$ in $\mathcal{I}_2$, with $t+1 \leq \varsigma \leq j$, $j << m$, and **Repeat** $(\mathcal{S}_\mathbf{1})'$ with the updated $\mathcal{I}_2$

If $|\mathcal{P}_{1,\varsigma} - \mathcal{P}_{0,\tau^0}| > \zeta$,
The first change location is estimated on $\tau_1 = m + t$.
Then, Go to **Location 2**.

Else
A **False Alarm** is detected.
Remove X_{m+t} from the sample, Do $t = t + 1$ and Go to $(\mathcal{S}_\mathbf{1})$.

Else
Do $t = t + 1$ and Go to $(\mathcal{S}_\mathbf{1})$.

Location 2 :

Consider the next h observations to X_{τ_1}: $X_{\tau_1+1}, \ldots, X_{\tau_1+h}$
Put $t = 1$ and Do

$(\mathcal{S}_\mathbf{2})$: Consider the two intervals $\mathcal{I}_1$ and $\mathcal{I}_2$ that contains respectively the observations $X_{\tau_1}, \ldots, X_{\tau_1+h+t-1}$ and $X_{\tau_1}, \ldots, X_{\tau_1+h+t}$. So that the difference between the two intervals considered is the single observation X_{τ_1+h+t} which is under testing.
$(\mathcal{S}_\mathbf{2})'$: **Adjust** model (31) to $\mathcal{I}_1$ and $\mathcal{I}_2$. Then, apply the testing procedure presented in Salman (2022).

If $|\mathcal{P}_{1,t} - \mathcal{P}_{0,\tau^0}| > \zeta$,

Replace X_{τ_1+h+t} with $X_{\tau_1+h+\varsigma}$ in $\mathcal{I}_2$, with $t+1 \leq \varsigma \leq j$, $j << h$, and **Repeat** $(\mathcal{S}_\mathbf{2})'$ with the updated $\mathcal{I}_2$

If $|\mathcal{P}_{1,\varsigma} - \mathcal{P}_{0,\tau^0}| > \zeta$,
The second change location is estimated on $\tau_2 = \tau_1 + h + t$
Then, Go to **Location 3**.

Else
A **False Alarm** is detected.
Remove X_{τ_1+h+t} from the sample, Do $t = t + 1$ and Go to $(\mathcal{S}_\mathbf{2})$.

Else
Do $t = t + 1$ and Go to $(\mathcal{S}_\mathbf{2})$.

Location i :

We already estimated the $(i-1)^{th}$ change location τ_{i-1} in step $i-1$
Consider the next h observations to $X_{\tau_{i-1}}$: $X_{\tau_{i-1}+1}, \ldots, X_{\tau_{i-1}+h}$
Put $t = 1$ and Do

$(\mathcal{S}_\mathbf{i})$: Consider the two intervals $\mathcal{I}_1$ and $\mathcal{I}_2$ that contains respectively the observations $X_{\tau_{i-1}}, \ldots, X_{\tau_{i-1}+h+t-1}$ and $X_{\tau_{i-1}}, \ldots, X_{\tau_{i-1}+h+t}$. So that the difference between the two intervals considered is the single observation under testing.
$(\mathcal{S}_\mathbf{i})'$: **Adjust** model (31) to $\mathcal{I}_1$ and $\mathcal{I}_2$. Then, apply the testing procedure presented in Salman (2022).

If $|\mathcal{P}_{1,t} - \mathcal{P}_{0,\tau^0}| > \zeta$,

Replace $X_{\tau_{i-1}+h+t}$ with $X_{\tau_{i-1}+h+\varsigma}$ in $\mathcal{I}_2$, with $t+1 \leq \varsigma \leq j$, $j << h$, and **Repeat** $(\mathcal{S}_\mathbf{i})'$ with the updated $\mathcal{I}_2$

If $|\mathcal{P}_{1,\varsigma} - \mathcal{P}_{0,\tau^0}| > \zeta$,

The i^{th} change location is estimated on $\tau_i = \tau_{i-1} + h + t$.
Then, Go to **Location** $i+1$.

Else

A **False Alarm** is detected.
Remove $X_{\tau_{i-1}+h+t}$ from the sample, Do $t = t+1$ and Go to $(\mathcal{S}_\mathbf{i})$.

Else

Do $t = t+1$ and Go to $(\mathcal{S}_\mathbf{i})$.

5 Simulation experiment

In this section, the theoretical results obtained in Salman (2022) are applied to some special simulated data, using softwares R and Python. Following the algorithm in Section 4, we detect weak changes and estimate their locations. By monitoring the values of the power of the test obtained around the estimated change, we distinguish if it is about a change-point or a false alarm.
Initially, we observe the power of the test computed through our algorithm to assess the occurrence of false alarms. Subsequently, we establish that the novel algorithm possesses the capability to differentiate between a change-point and a false alarm, relying on the power's behavior calculated in the vicinity of the detected change. Furthermore, we evaluate the efficiency of our algorithm for detecting multiple weak breaks where the number of change-point and their locations are assumed to be unknown. At the same time, we evaluate if the changes locations estimation are more accurate than the others obtained in Salman (2022) by taking the same parameters values as in Salman (2022).
For the simulation, we use the same particular CHARN model as in Salman (2022) having the following expression

$$X_t = \rho_{0,1} + \frac{\beta_{j,1}}{\sqrt{n}} + \left(\rho_{0,2} + \frac{\beta_{j,2}}{\sqrt{n}}\right) X_{t-1}\, e^{\left(\rho_{0,3} + \frac{\beta_{j,3}}{\sqrt{n}}\right) X_{t-1}^2} + \sqrt{\theta_1 + \theta_2 X_{t-1}^2}\,\varepsilon_t, \quad j = 1, \ldots, k, \quad t \in \mathbb{Z}, \quad (55)$$

where n denotes the number of observations, $(\varepsilon_t)_t$ is a standard white noise with a differentiable density f. Here, on $[\tau_{j-1}, \tau_j)$, $\boldsymbol{\rho}_0 = (\rho_{0,1}, \rho_{0,2}, \rho_{0,3}) \in \mathbb{R}^3$, $\boldsymbol{\beta}_j = (\beta_{j,1}, \beta_{j,2}, \beta_{j,3}) \in \mathbb{R}^3$; $\boldsymbol{\rho}_0$ is the parameter to be specified in each particular model considered.

5.1 Data presenting one single False Alarm

In this part, we consider the problem of detecting and identifying a change. Identifying a change means that we distinguish between a false alarm and a change-point basing on the power calculated around the estimate change. The data are generated by model (55) for $\rho_{0,1} = 0.2$, $\rho_{0,2} = 0.3$ and $\rho_{0,3} = \beta_{1,1} = \beta_{1,2} = \beta_{1,3} = 0$ (same parameter values token in those papers). At an instant between 1 and n, say τ_1, we replace the corresponding observation, say X_{τ_1}, by another observation, for example ϵ that follows $\mathcal{N}(1,3)$. For $\zeta = 0.4\%$, $\alpha = 5\%$ and $\tau_1 = 150$, the results corresponding are shown on Figure 1. From Figure 1, one can see that the power of the test jumps above the threshold at $t = 150$ (the threshold here is $\alpha + \zeta = 5.4\%$), which is the true instant of change, and directly it fell under the threshold for the next few observations. For different τ_1, we monitor the power of the test calculated at $\tau_1 + i$, $i = -1, 0, \ldots, 4$. The results are shown on Table 1 and they illustrate numerically what we said about Figure 1.
One can see that the power calculated at $\tau_1 + i$, $i = 1, 2, 3, 4$ are higher than the others before τ_1 which is normal, because we calculated them by removing the intermediate observation at the estimates τ_1, and this thing affect the estimation of the possible autocorrelation parameters between the last two observations in $\mathcal{I}_2$ (see Section 4). Also, by comparing these powers to that at $\widehat{\tau}_1$, we can see that they are much less, which lead us to classifying this change as a false alarm.

Power	τ_1			
	90	110	150	195
$\widehat{\tau}_1$	90	110	150	195
$\mathcal{P}_{1,\widehat{\tau}_1-1}$	0.05099	0.05124	0.05091	0.05071
$\mathcal{P}_{1,\widehat{\tau}_1}$	0.05612	0.05721	0.05851	0.05762
$\mathcal{P}_{1,\widehat{\tau}_1+1}$	0.05218	0.05181	0.05213	0.05213
$\mathcal{P}_{1,\widehat{\tau}_1+2}$	0.05232	0.05194	0.05273	0.05224
$\mathcal{P}_{1,\widehat{\tau}_1+3}$	0.05212	0.05174	0.05283	0.05211
$\mathcal{P}_{1,\widehat{\tau}_1+4}$	0.05234	0.05179	0.05255	0.05215

Table 1: Power of the test around τ_1 for $\zeta = 0.4\%$ and $\alpha = 5\%$.

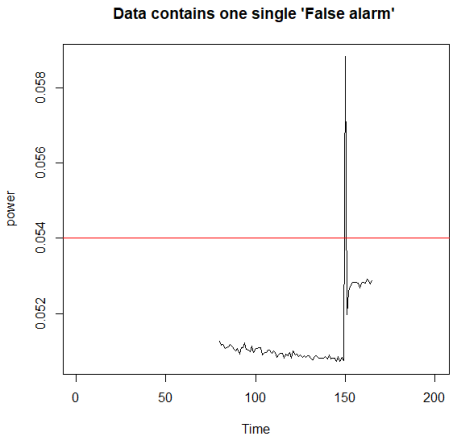

Fig. 1: Estimation of the change location for $\tau_1 = 150$ in a class of AR(1) models.

In the same line, we consider the problem of detecting changes, estimating their locations and identifying their type. For that, we generate a data that present one single change-point and one single false alarm using the following particular case of model (55)

$$\begin{cases} X_t = & \rho_{0,1} + \rho_{0,2} X_{t-1} + \varepsilon_t, & t = 1, \dots, \tau_1 - 1, \\ X_t = & \rho_{0,1} + \dfrac{\beta_{1,1}}{\sqrt{n}} + \left(\rho_{0,2} + \dfrac{\beta_{1,2}}{\sqrt{n}}\right) X_{t-1} + \varepsilon_t, & t = \tau_1, \dots, n \\ X_{\tau_2} = & \epsilon, & \end{cases}$$

where $(\varepsilon_t)_{t\geq 1}$ is a standard Gaussian white noise and ϵ is a Gaussian random variable with different parameters values.
For $n = 300$, $\rho_{0,1} = 0.2$, $\rho_{0,2} = 0.3$, $\beta_{1,1} = 5$, $\beta_{1,2} = -3$, $\epsilon \sim \mathcal{N}(-1, 2)$ and $\zeta = 0.25\%$, Figure 2 illustrates the behavior of the power when facing a change. Now, for $n = 300$, $\rho_{0,1} = 0.2$, $\rho_{0,2} = 0.3$, Table 2 shows the estimation of the break locations corresponding to different type and magnitudes of changes, and different values of ζ.

$\widehat{\tau}$ and power	$((\beta_{11}, \beta_{1,2}), (\tau_1, \tau_2), \epsilon \sim, \zeta))^\top$			
	$(1,1)$ $(101, 200)$ $\mathcal{N}(1,1)$ 0.15%	$(3,-2)$ $(101, 250)$ $\mathcal{N}(1,2)$ 0.25%	$(5,-3)$ $(111, 280)$ $\mathcal{N}(-1,2)$ 0.25%	$(10,-6)$ $(91, 295)$ $\mathcal{N}(2,2)$ 0.35%
$\widehat{\tau}_1$	102	101	111	91
$\mathcal{P}_{1,\tau_1-1}$	0.050541	0.050713	0.050811	0.050972
$\mathcal{P}_{1,\tau_1}$	0.052418	0.053712	0.054612	0.057321
$\mathcal{P}_{1,\tau_1+1}$	0.052503	0.053515	0.054874	0.057819
$\mathcal{P}_{1,\tau_1+2}$	0.052315	0.053821	0.054731	0.057643
$\mathcal{P}_{1,\tau_1+3}$	0.052517	0.053644	0.054912	0.057967
$\mathcal{P}_{1,\tau_1+4}$	0.052421	0.053553	0.054826	0.058042
$\widehat{\tau}_2$	200	250	280	295
$\mathcal{P}_{2,\tau_2-1}$	0.050912	0.050626	0.050963	0.050121
$\mathcal{P}_{2,\tau_2}$	0.052915	0.054261	0.053987	0.061092
$\mathcal{P}_{2,\tau_2+1}$	0.051981	0.051725	0.516471	0.051681
$\mathcal{P}_{2,\tau_2+2}$	0.051734	0.051628	0.051811	0.051874
$\mathcal{P}_{2,\tau_2+3}$	0.051413	0.051632	0.051736	0.051642
$\mathcal{P}_{2,\tau_2+4}$	0.051386	0.051589	0.051481	0.051328

Table 2: Power around changes detected in a class of AR(1) model.

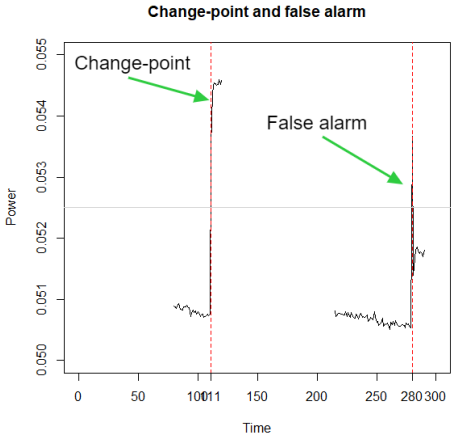

Fig. 2: Behavior of the power when facing a change.

5.2 Multiple change-points detection (k=3)

In this part, we consider the problem of detecting multiple change-points in class of non-linear models, such as AR(1)-ARCH(1) model which is a particular class of CHARN(1,1) models. We use the same values

of the parameters used in Salman (2022) in order to compare the results, efficiency and accuracy between the results obtained by that algorithm and those obtained by the new version introduced in this paper. In addition, for each detecting change, we monitor the power calculated at some instants around estimates instant of change in order to identify the type of the change detected.
We consider the data generated by model (55), for $\tau = (\tau_1, \tau_2, \tau_3)$ represents the true instant of changes, $n = 350, \rho_{0,1} = 0.2$, $\rho_{0,2} = 0.3$, $\rho_{0,3} = \beta_{j,3} = 0$, $j = 1, 2, 3$, $\theta_1 = 1$, $\theta_2 = 0.02$. For 5000 replications, different magnitudes of change $\beta_j = (\beta_{j,1}, \beta_{j,2})$, $j = 1, 2, 3$ and same $\zeta = 0.1\%$, the results are shown on Table 3.

$\tau = (\tau_1, \tau_2, \tau_3) = (90, 190, 275)$			
Power	$\begin{pmatrix} \beta_{1,1} & \beta_{1,2} \\ \beta_{2,1} & \beta_{2,2} \\ \beta_{3,1} & \beta_{3,2} \end{pmatrix}$		
	$\begin{pmatrix} 3 & 2 \\ 1 & 3 \\ -1 & 1 \end{pmatrix}$	$\begin{pmatrix} 1 & -0.5 \\ 2 & 1 \\ -1 & -1 \end{pmatrix}$	$\begin{pmatrix} -2 & 1.5 \\ 1 & 3 \\ -0.5 & -1 \end{pmatrix}$
$\widehat{\tau}_1$	90	91	91
$\mathcal{P}_{1,\tau_1-1}$	0.050342	0.050214	0.050312
$\mathcal{P}_{1,\tau_1}$	0.052117	0.051917	0.052162
$\mathcal{P}_{1,\tau_1+1}$	0.052313	0.052023	0.052213
$\mathcal{P}_{1,\tau_1+2}$	0.052325	0.051976	0.051909
$\mathcal{P}_{1,\tau_1+3}$	0.052318	0.052014	0.052132
$\mathcal{P}_{1,\tau_1+4}$	0.052510	0.052134	0.052193
$\widehat{\tau}_2$	191	191	190
$\mathcal{P}_{2,\tau_2-1}$	0.050314	0.050352	0.050963
$\mathcal{P}_{2,\tau_2}$	0.052203	0.052134	0.053102
$\mathcal{P}_{2,\tau_2+1}$	0.052491	0.052232	0.528902
$\mathcal{P}_{2,\tau_2+2}$	0.051908	0.052109	0.052932
$\mathcal{P}_{2,\tau_2+3}$	0.052424	0.052421	0.053011
$\mathcal{P}_{2,\tau_2+4}$	0.052521	0.051996	0.053106
$\widehat{\tau}_3$	276	276	275
$\mathcal{P}_{3,\tau_3-1}$	0.050142	0.050324	0.050561
$\mathcal{P}_{3,\tau_3}$	0.052722	0.053341	0.053978
$\mathcal{P}_{3,\tau_3+1}$	0.052524	0.053242	0.538511
$\mathcal{P}_{3,\tau_3+2}$	0.052498	0.053234	0.053915
$\mathcal{P}_{3,\tau_3+3}$	0.052713	0.053517	0.053776
$\mathcal{P}_{3,\tau_3+4}$	0.052613	0.053127	0.053817

Table 3: Power around changes detected in a class of AR(1)-ARCH(1) model.

One can see from Table 3 that the results is more accurate than those obtained in Salman (2022). In addition, for a suitable threshold corresponding to a suitable ζ, it is rarely that we find a detection change in advance of the real instant of break from which it was removed during the replications. This feature is a result of the newly introduced algorithm version here, which reduces the impact of white noise.

6 Welding electrical signals

Welding is considered the main task for many industries, especially for those that construct hot water tanks. The problem of detecting and locating a fault welding is considered as one of the most important problems for quality evaluation. Using welding electrical signals as data source, many research have been done for welding fault detection. Huang et al. (2020) detects three types of defects by proposing a Support Vector Machine (SVM) model based on the multi-scale entropy of the current and voltage signals. Pernambuco et al. (2019) classify the sound signals to detect the absence of shielding gas using Artificial Neural Network.

From time series of view, Melakhsou and Batton-Hubert (2021) propose a method that detects and localize welding defect based on the findings from causality study knowing that the causality between time series has begun with Kamiński et al. (2001).
The change in the mean WES is mainly caused by the change in the distance between the electrode and the surface under welds. That means, since the electrode is fixed, it is an indicator of the variation of the circular surface form of the metal under welds. This variation may be due to a fault during the transformation of the metal plate to a cylinder, or the existence of a hole.
Here, our global purpose is to test for weak changes in the mean of some arc-welding series that considered as a "normal welding series" in order to monitor the stability of the electrical signals. The data that we have are for 10 normal welds experiments under the same conditions. We study all of these data and we present the results of four of them.

6.1 Modeling

First, we start our study by looking for a common suitable time series model for all of these data. The chronogram of the EWS series (W_t) (Figure 3) seems to present a trend and does not present a seasonality. The Augmented Dicky-Fuller test (see Cheung and Lai (1995)) approve the non-stationarity of all these data. The results obtained in Salman (2022) cannot be used directly, since the Moving-Average part doesn't belongs to the class of CHARN models used there. For that, we decompose these series in a summation of two components as follow:

$$W_t = Y_t + X_t,$$

where (Y_t) represents the unknown trend assumed to be continuous and (X_t) is a piece-wise stationary series with mean (μ_t) and variance (σ_t). Based on the lowest Akaike Information criterion AIC (see Sakamoto et al. (1986)), we estimate the trend by the following moving-average with order 5

$$\widehat{Y_t} = \frac{1}{5}\sum_{j=-2}^{2} W_{t+j}.$$

The Box-Ljung and Box-Pierce tests (see Brockwell and Davis (2002)) applied to these residuals series reject the null hypotheses, and then they are not iid. Also, the QQ-plot and the histogram of the residuals seems to explain that the residuals is normally distributed in addition to Shapiro-wilk test. Basing on all of these investigations, we assume the heteroscedasticity of these residual series and by taking into consideration the AIC, we propose a shifted model defined as follow

$$X_t = \rho_{0,1} + \frac{\beta_{j,1}}{\sqrt{n}} + \sigma_j \varepsilon_t, \quad t \in [\tau_{j-1}, \tau_j), \quad j = 1, \ldots, k+1,$$

where k is the number of change-points that assumed to be unknown and must be estimated, $\tau_1, \ldots, \tau_k$ designate the breaks locations, (ε_t) is a standard Gaussian white noise, $V(x) = \sigma_j$ represents the variance of X_t in each interval $[\tau_{j-1}, \tau_j)$.
Here, for the test problem, $\boldsymbol{\gamma}_0 = 0$, $\boldsymbol{\gamma}_n = (0, \beta_2/\sqrt{n}, \ldots, \beta_{k+1}/\sqrt{n}) \in \mathbb{R}^{k+1}$ with $\boldsymbol{\beta} = (0, \beta_2, \ldots, \beta_{k+1})$.
Using the theoretical results of Salman (2022) recalled in Section 3, and by applying our new version algorithm presented in Section 4, for different thresholds corresponding to the choice of ζ, we detect multiple breaks in the data and we show the results of 4 of them for $\zeta = 0.15\%$, 0.25%, and 0.3% on Figure 3.

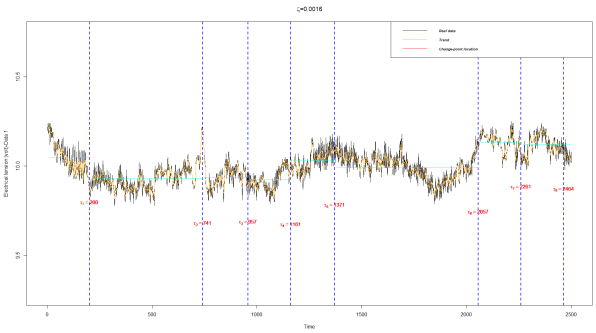

(a) Data 1 and $\zeta = 0.15\%$.

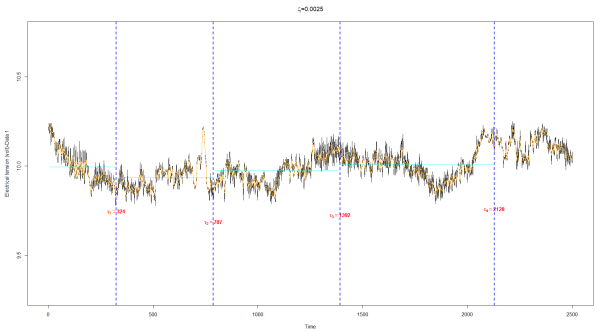

(b) Data 1 and $\zeta = 0.25\%$.

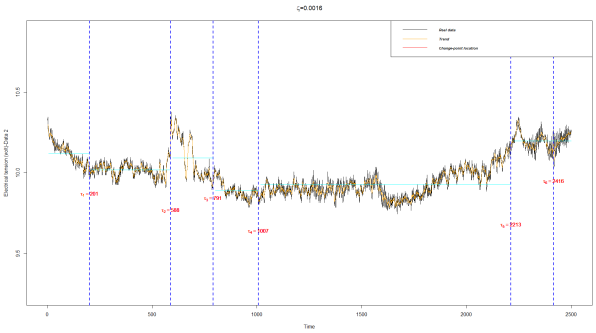

(c) Data 2 and $\zeta = 0.15\%$.

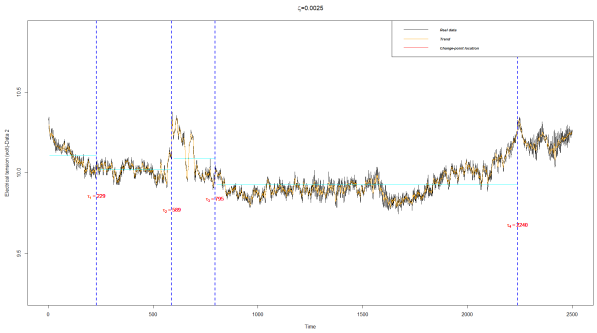

(d) Data 2 and $\zeta = 0.25\%$.

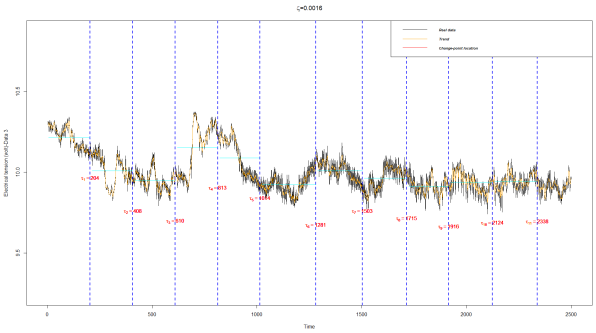

(e) Data 3 and $\zeta = 0.15\%$.

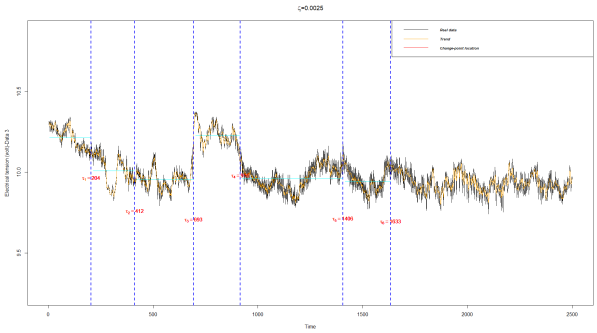

(f) Data 3 and $\zeta = 0.25\%$.

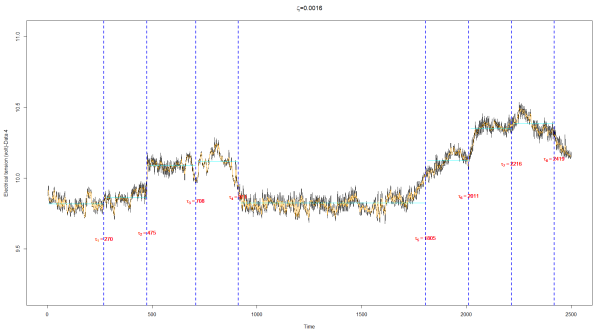

(g) Data 4 and $\zeta = 0.15\%$.

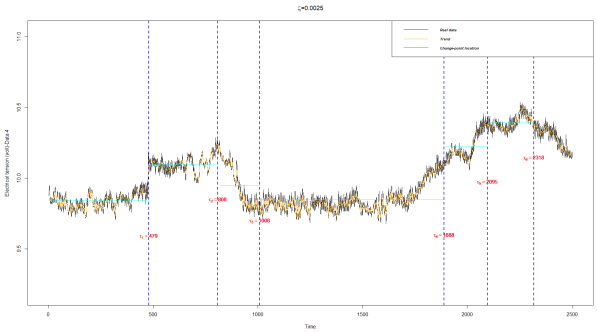

(h) Data 4 and $\zeta = 0.25\%$.

Fig. 3: Breaks locations estimation in case of $\zeta = 0.15\%$ and 0.25%.

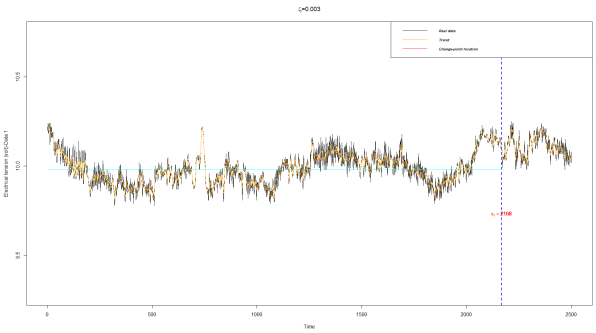

(a) Data 1 and $\zeta = 0.3\%$.

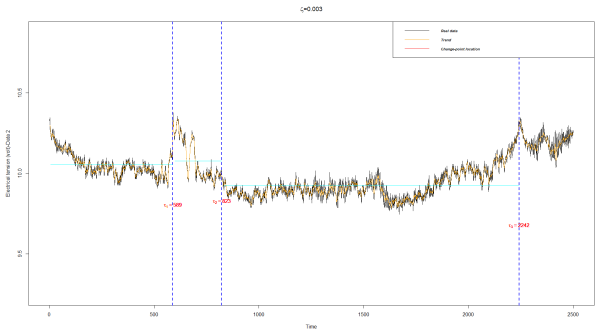

(b) Data 2 and $\zeta = 0.3\%$.

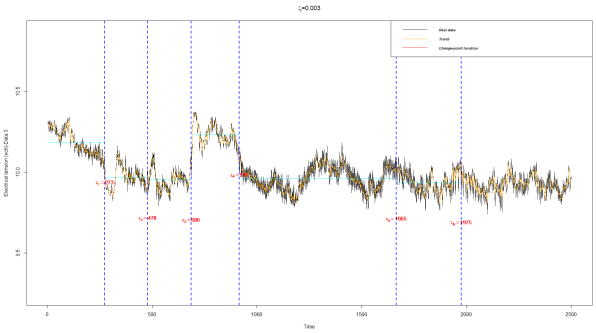

(c) Data 3 and $\zeta = 0.3\%$.

(d) Data 4 and $\zeta = 0.3\%$.

Fig. 4: Breaks locations estimation in case of $\zeta = 0.15\%$ and 0.25%

Now, since all of these data are considered as a normal welding, it is interesting to take a look to the variation of the number of changes detected with respect to the threshold. For that, we consider a sequence of ζ varying between 0.15% and 1%, we applied our algorithm on each data for each value of ζ and we calculate the corresponding number of changes detected. The results are shown on Figure 5.

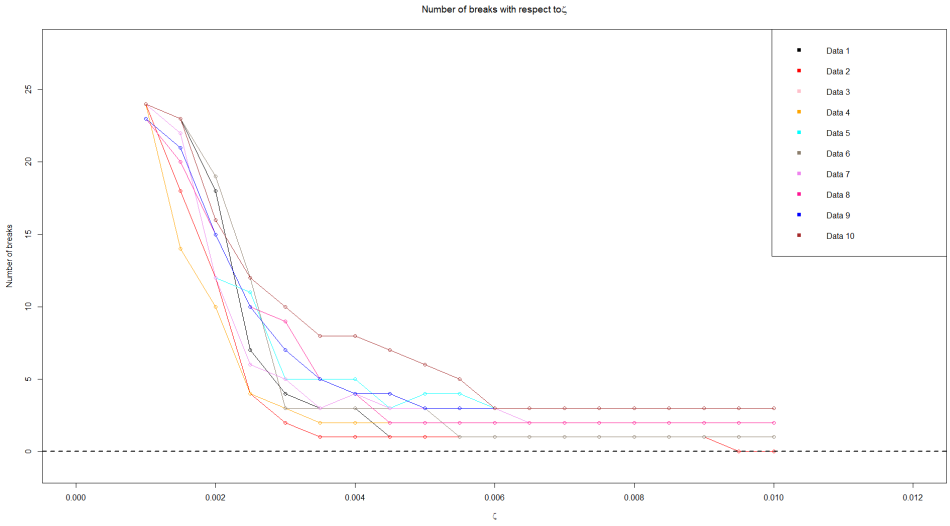

Fig. 5: Number of breaks with respect to ζ.

6.2 Analyses

For these 10 data, we applied our algorithm for ζ varying between 0.1% and 1%. For $0.1\% \leq \zeta \leq 0.13\%$, a high number of weak breaks has been detected which is not an informative phenomenon in this domain. Figure 3 and 4 shows the corresponding breaks detected of four of these data for $\zeta = 0.15\%$, 0.25% and 0.3%. It is easy to see that the number of changes detected decrease when the threshold increase which

is logic, and also, some estimated breaks locations remains close to each other even when we change the threshold. For example, in Data 2, the instant $t = 589$ remains the same instant detected when $\zeta = 0.15\%$ or 0.3% from which we can consider it as a true change.
Also, for all of these data, when a change is detected, the power remains above the threshold except the case of that corresponding to Data 2 where, for $\zeta = 0.25\%, 0.3\%$, the instant $t = 2245$ is considered as a false alarm and it can be explained here by a hole.
These results allows us to assume the segmentation of the data into piece-wise stationary data from which the distance between the observations that belong to every single piece and the electrode is significantly constant. One can see that, by fixing a threshold, we can find the reason that make the distance between the electrode and the surface metal plat under welds change. By monitoring the values of the power of the test, we can classify the changes detected into a deformation of the circular form of the hot water tank or a hole. In other word, the false alarm definition introduced in Section 4 can be explained here as a hole from which the power cross the threshold for a few number of observations, and the true change as the point where the deformation of the circular form started.
From Figure 5, we can see that the number of breaks detected decrease exponentially when ζ is varying between 0.15% and 0.35% and then, it remains constant for a while before converging to zero. We can explain this fall of the number of changes detected through the weak variation of the values of the welding signals from which the power of the test cross the threshold for a small ζ and it remains under the threshold for a higher ζ. In addition, by taking $\zeta = 9\%$, no change has been detected in all of these data.

7 Conclusion

We have introduced a new automatic algorithm for detecting weak changes in the mean using the method proposed by Salman (2022). The simulation experiment conducted shows that our algorithm is efficient to detect multiple breaks, and also, to distinguish between a change-point and false alarm. Comparing to the results obtained in Salman (2022), our algorithm seems to be more efficient and accurate.
By applying the theoretical results of Salman (2022) with the algorithm proposed here, we detect multiple weak changes in the welding electrical signals in order to study the stability of the electrical tension during the construction of hot water tank.
An aspect of our outlook, pertaining to this study, involves devising an automated approach to determine the optimal threshold suitable for the specific domain of investigation. Addressing this global challenge is a paramount concern for numerous researchers in this field, and it stands as a significant focus for our forthcoming endeavors.

References

Andreou, E. and Ghysels, E. (2009). Structural breaks in financial time series. *Handbook of financial time series*, pages 839–870.

Aue, A. and Horváth, L. (2013). Structural breaks in time series. *Journal of Time Series Analysis*, 34(1):1–16.

Beaulieu, C., Chen, J., and Sarmiento, J. L. (2012). Change-point analysis as a tool to detect abrupt climate variations. *Philosophical Transactions of the Royal Society A: Mathematical, Physical and Engineering Sciences*, 370(1962):1228–1249.

Brockwell, P., Davis, R., and Salehi, H. (1990). A state-space approach to transfer-function modeling. *Statistical Inference in Stochastic Processes*, 6:233.

Brockwell, P. J. and Davis, R. A. (2002). *Introduction to time series and forecasting*. Springer.

Brown, R. L., Durbin, J., and Evans, J. M. (1975). Techniques for testing the constancy of regression relationships over time. *Journal of the Royal Statistical Society: Series B (Methodological)*, 37(2):149–163.

Chen, G.-y., Gan, M., and Chen, G.-l. (2018). Generalized exponential autoregressive models for nonlinear time series: stationarity, estimation and applications. *Information Sciences*, 438:46–57.

Cheung, Y.-W. and Lai, K. S. (1995). Lag order and critical values of the augmented dickey–fuller test. *Journal of Business & Economic Statistics*, 13(3):277–280.

Cho, H. and Fryzlewicz, P. (2012). Multiscale and multilevel technique for consistent segmentation of nonstationary time series. *Statistica Sinica*, pages 207–229.

Davis, R. A., Lee, T. C. M., and Rodriguez-Yam, G. A. (2006). Structural break estimation for nonstationary time series models. *Journal of the American Statistical Association*, 101(473):223–239.

Droesbeke and Fine, J.-J. (1996). *Inférence non paramétrique: Les statistiques de rangs*. Ed. de l'Université de Bruxelles; Ed. Ellipses.

Fryzlewicz, P. (2014). Wild binary segmentation for multiple change-point detection. *The Annals of Statistics*, 42(6):2243–2281.

Härdle, W., Tsybakov, A., and Yang, L. (1998). Nonparametric vector autoregression. *Journal of Statistical Planning and Inference*, 68(2):221–245.

Horváth, L. (1993). The maximum likelihood method for testing changes in the parameters of normal observations. *The Annals of statistics*, pages 671–680.

Horváth, L., Miller, C., and Rice, G. (2020). A new class of change point test statistics of rényi type. *Journal of Business & Economic Statistics*, 38(3):570–579.

Huang, Y., Yang, D., Wang, K., Wang, L., and Zhou, Q. (2020). Stability analysis of gmaw based on multi-scale entropy and genetic optimized support vector machine. *Measurement*, 151:107282.

Kamiński, M., Ding, M., Truccolo, W. A., and Bressler, S. L. (2001). Evaluating causal relations in neural systems: Granger causality, directed transfer function and statistical assessment of significance. *Biological cybernetics*, 85:145–157.

Killick, R., Fearnhead, P., and Eckley, I. A. (2012). Optimal detection of changepoints with a linear computational cost. *Journal of the American Statistical Association*, 107(500):1590–1598.

Korkas, K. K. and PryzlewiczV, P. (2017). Multiple change-point detection for non-stationary time series using wild binary segmentation. *Statistica Sinica*, pages 287–311.

Le Cam, L. (1986). The central limit theorem around 1935. *Statistical science*, pages 78–91.

Ltaifa, M. (2021). *Tests optimaux pour détecter les signaux faibles dans les séries chronologiques*. Theses, Université de Lorraine ; Université de Sousse (Tunisie).

Melakhsou, A. A. and Batton-Hubert, M. (2021). On welding defect detection and causalities between welding signals. In *2021 IEEE 17th International Conference on Automation Science and Engineering (CASE)*, pages 401–408. IEEE.

Ngatchou-Wandji, J. and Ltaifa, M. (2021). On detecting weak changes in the mean of charn models. *arXiv preprint arXiv:2101.08597*.

Page, E. S. (1954). Continuous inspection schemes. *Biometrika*, 41(1/2):100–115.

Pernambuco, B. S. G., Steffens, C. R., Pereira, J. R., Werhli, A. V., Azzolin, R. Z., and Estrada, E. d. S. D. (2019). Online sound based arc-welding defect detection using artificial neural networks. In *2019 Latin American robotics symposium (LARS), 2019 Brazilian symposium on robotics (SBR) and 2019 workshop on robotics in education (WRE)*, pages 263–268. IEEE.

Perron, P. et al. (2006). Dealing with structural breaks. *Palgrave handbook of econometrics*, 1(2):278–352.

Reeves, J., Chen, J., Wang, X. L., Lund, R., and Lu, Q. Q. (2007). A review and comparison of changepoint detection techniques for climate data. *Journal of applied meteorology and climatology*, 46(6):900–915.

Sakamoto, Y., Ishiguro, M., and Kitagawa, G. (1986). Akaike information criterion statistics. *Dordrecht, The Netherlands: D. Reidel*, 81(10.5555):26853.

Salman, Y. (2022). *Testing a class of time-varying coefficients CHARN models with application to change-point study*. PhD thesis, Lorraine University; Lebanese University.

Stoumbos, Z. G., Reynolds Jr, M. R., Ryan, T. P., and Woodall, W. H. (2000). The state of statistical process control as we proceed into the 21st century. *Journal of the American Statistical Association*, 95(451):992–998.

Vostrikova, L. Y. (1981). Detecting "disorder" in multidimensional random processes. In *Doklady akademii nauk*, volume 259, pages 270–274. Russian Academy of Sciences.

Yao, Y.-C. (1987). Approximating the distribution of the maximum likelihood estimate of the change-point in a sequence of independent random variables. *The Annals of Statistics*, pages 1321–1328.

Yau, C. Y. and Zhao, Z. (2016). Inference for multiple change points in time series via likelihood ratio scan statistics. *Journal of the Royal Statistical Society: Series B (Statistical Methodology)*, 78(4):895–916.

Zeileis, A. (2001). p values and alternative boundaries for cusum tests. Technical report, Technical Report.

Zeileis, A. (2004). Alternative boundaries for cusum tests. *Statistical Papers*, 45(1):123–131.